Transient variations of vertical total electron content at low latitude during the period 2013–2017

Ali O Hammou, N. Zaourar, R. Fleury, C. Amory-Mazaudier

Transient variations of vertical total electron content at low latitude during the period 2013- 2017

Hammou Ali O.[1], Zaourar N.[1], Fleury R.[2], Amory-Mazaudier C.[3,4]

1. Geophysical Laboratory, FSTGAT, B.P.32 USTHB, 16123 Bab-Ezzouar, Algeria
2. Lab.-STICC, UMR CNRS 6285, Institut Mines-Telecom CS, 83818 Brest cedex 3, France
3. LPP, CNRS/Ecole Polytechnique/Sorbonne Université/Université Paris-Sud/Observatoire de Paris, 75006 Paris, France
4. T/ICT4D, ICTP, International Centre for Theoretical Physics, Strada Costiera, 11, I – 34151, Italy (omar.hammouali47@gmail.com)

Abstract

We use GPS networks to measure the vertical Total Electron Content (VTEC) variations at low latitude, in three longitude sectors: America, Europe-Africa and Asia, collected during the period 2013 – 2017. This period corresponds to the increasing phase of the solar cycle 24 (SC#24) observed around 2013-2014 as well as the decreasing phase around 2014-2017. Our results discussed a morphological analysis of regular variations in ionization during different phases of solar activity: daytime variations, seasonal and semi-annual variations and variations based on the solar cycle 24 in three longitude sectors. In all longitude sectors, the highest VTEC values are displayed during the two months of the spring, located after sunrise and before sunset. The lowest values are found during the summer and winter seasons. We found that the winter anomaly and the presence of equinoxial peaks are the most pronounced effects in VTECs in the increasing and decreasing phase of the SC#24. A strong asymmetry is detected between equinoxial peaks and the location of peaks occurring in March/April and October/November at maximum in the solar flux variations during the increase phase. We show that the daily VTEC maximum values were registered between 14:00 and 16:00 LT and the minimum values between 4:00 and 6:00 LT. Double ionization peak in the morning and evening is observed in VTEC annual variations, due to the proximity of the equatorial fountain stations. From the statistical analysis part, we observed practically the same distribution of the different classes of VTEC (two peaks, bell-shaped and plateau-shaped) variations in the three sectors of longitude. These observations indicate longitudinal variation in the presence of the winter anomaly in the Equatorial Ionized Anomaly (EIA) region. Additionally, we can note a longitudinal variation of the spring-autumn VTEC asymmetry in the EIA region during the five years 2013-2017. We observe also that the occurrence of nocturnal peak recorded around 19 local time (LT) shows the same characteristics as the vertical drift E x B (B: magnetic field is perpendicular to E: electric field.) with respect to solar cycle, season and longitude. Three essential characteristics we noted: 1) the occurrence of the nocturnal peak generally follows the solar cycle. 2) The occurrence of the nocturnal peak is generally stronger at the equinoxes than at the solstices. 3) The occurrence of the nocturnal peak is stronger in the Europe-Africa and America sectors than in the Asia sector. As a result, nocturnal peak occurrence is well related to the PRE at the origin of the GNSS signal scintillations.

Keywords: Ionosphere at low latitude, GPS, TEC, ionization.

1. Introduction

The ionosphere is the ionized layer of the Earth's atmosphere between (50-1000) km initiated by ultraviolet (UV), extreme ultraviolet (EUV) and X-rays solar radiations. The Ionosphere is extremely variable according to altitude, latitude, longitude, local time, season, sunspot cycle, and magnetic activity. The characteristic phenomenon of the equatorial zone is the Equatorial Fountain creating the Equatorial Ionization Anomaly (EIA). The equatorial fountain EIA, first discovered by (Namba and Maeda, 1939;

Appleton, 1946) is due to the fact that the magnetic field is horizontal at the equator. And, as a consequence, the E x B drift due to an eastward electric field (Lorentz force) is vertical and drives the plasma upward during the daytime. At low altitudes, the Lorentz force is the dominant force and the plasma move up. At highest altitudes, where the pressure gradient and the gravity forces become significant the plasma is driven by the ambipolar diffusion through the magnetic field lines and there is the creation of the EIA. A trough of density at the equator and two peaks of density in the geomagnetic latitudes around 15°/20° N and 15°/20° S compose the EIA. The eastward electric field, causing E x B during the day, increases strongly just before sunset and becomes westward. This phenomenon is called PRE: Pre Reversal Enhancement. The westward E x B moves down the plasma. The existence of equatorial plasma irregularities (EPB) is attributed to the Generalized Rayleigh-Taylor (RT) plasma instability related to the PRE (Fejer et al., 1999; Kelley, 2009). The PRE was first observed at Jicamarca by Woodman (1970). Another characteristic of the equatorial region is the existence of the Equatorial Electrojet (EEJ).The EEJ is an electric current flowing in the E-region of the ionosphere (~110km), along the magnetic equator, between 3°N and 3°S geomagnetic latitude (Chapman, 1951; Amory-Mazaudier et al., 1993). The EIA is the main phenomena affecting equatorial latitudes. The EIA is controlled by the electric field, neutral wind and magnetic declination between the magnetic and geographical equator. The effect of EIA on the variation of the TEC depends on the seasons, local time, and the most important parameter is magnetic latitude. Recent studies (Le et al., 2013; Bilitza et al., 2017; Fang et al., 2018) indicate that there are ionospheric effects strongly due to seasonal variation and variation with longitude (local time) . The recent satellite produced detailed information on the morphology of the low latitude ionosphere (Fejer et al., 1995; Immel et al., 2006; Fejer et al., 2008; Jin et al., 2017; Olsen et al., 2016). A number of studies have been conducted at low latitude in the African sector on the variation in the critical frequency of foF2 (Adohi et al., 2008; Oladipo et al., 2008; Ouattara et al., 2009; Ouattara & Amory-Mazaudier, 2012; Thiam et al., 2012). In this article, we focus on diurnal, seasonal and solar variations in VTEC activity during five years of study (2013-2017) at low latitude in three longitude sectors, which corresponds to the increasing phase of the solar cycle 24 observed around 2013-2014 and the decreasing phase around 2014-2017. Section 2 describes of the database, data processing and the characteristics of our data sample. Section 3 presents the solar cycle, seasonal and diurnal VTEC variations at low latitude. Section 4 is devoted to statistical analysis on the shape of the VTEC, the amplitude of VTEC as a function of the season and the night-time enhancement of VTEC related to the PRE and we finally finish by a conclusion.

2. GPS data and GPS data processing

We analyzed the VTEC derived from 19 GPS receivers at low latitude (+40°, -40° geographic), located in the three longitude sectors America: 4 stations, Europe-Africa: 7 stations and Asia : 8 stations, during the period from 2013 to 2017. The stations were selected on the basis of the number of measurements available over the period studied 2013-2017. Figure 1 shows the distribution of the GPS stations around the magnetic equator. Table 1 gives the geographic and geomagnetic coordinates of the stations.

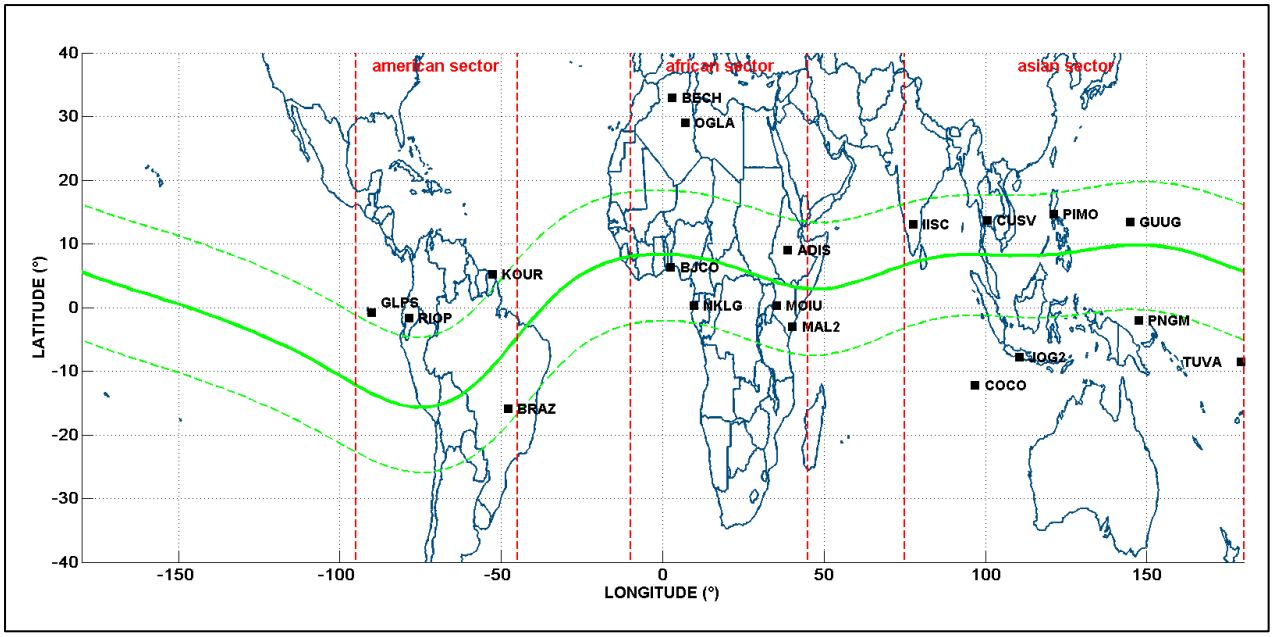

Fig 1. Geographic and geomagnetic coordinates of 21GPS stations.

Table 1. Geographic and geomagnetic coordinates (°) of the 19 GPS station

Site	Country	Geographic Latitude	Geographic Longitude	Modif_Dipole	UT/LT
		American Sector			
BRAZ	Brazil	-15,95	-47,88	-10.35	-3
GLPS	Equateur	-0,74	-90,3	9.84	-6
RIOP	Ecuador	-1,65	-78,65	10.38	-5
KOUR	French Guyana	5.25	-52.51	10.60	-3
		Europe-African Sector			
ADIS	Ethiopia	9,04	38,77	0.70	2
BJCO	Benin	6,38	2,45	-5.64	0
MAL2	Kenya	-3	40,19	-14.07	2
MOIU	Kenya	0,29	35,29	-10.70	2
NKLG	Gabon	0,35	9,67	-13.40	0
BECH	Algeria	33	3	25.17	0
OGLA	Algeria	29	7	25.86	0
		Asian Sector			
COCO	Australia	-12,19	96,83	-25.51	6
CUSV	Thailand	13,74	100,53	6.49	6
GUUG	USA	13,43	144,8	5.88	9
IISC	India	13,02	77,57	5.94	5
JOG2	Indonesia	-7,764	110,37	-18.74	7
PIMO	Philippines	14,64	121,08	7.72	8
PNGM	Papua Guiney	-2,04	147,37	-10.20	9
TUVA	Tuvalu	-8,53	179,2	-11.89	1

2.1 Processing

The GPS satellites circling the Earth at high altitude 20,200 km over the Earth's surface will provide data (pseudorange and carrier phase) to compute TEC which is the total number of electrons integrated in the path from the receiver to each GPS satellite. The Slant TEC is expressed by:

$$\mathrm{STEC} = \int_{R}^{S} \mathrm{N_e(s)}\ \mathrm{ds}$$

Where Ne: electron density, R: receiver altitude and S: satellite altitude. By (Klobuchar, 1996), it is impracticable to have the absolute value of the TEC, but on the other hand we can estimate an accurate estimate of the value of the TEC. GPS receivers provide both L-carrier phase delays and pseudo-P ranges of dual frequencies. We have two methods to calculate the relative phase delay between the two carrier frequencies: the (1st) pseudo-distance method gives an absolute scale of TEC with less precision, and the 2nd differential phase method, which increases the accuracy of the measurement but does not allow to know the number of phase cycles (Klobuchar, 1996). We follow Sardon et al.(1994) by removing differential instrumental biases because satellites and receivers for observable GPS are biased towards instrumental delays (Ya'acob et al., 2009). The Differential Code Bias (DCB) satellite biases used in this paper have been published daily by the international bodies of the Analysis Centre's (AC) dealing with positioning: Centre for the Determination of the European Orbit (CODE) (ftp://ftp.unibe.ch/aiub/CODE/). The fundamental GPS frequency is f1 and f2, defined as group delay:

$$TEC = \frac{(P_1 - P_2)}{40.3}\left(\frac{f_1^2 f_2^2}{f_2^2 - f_1^2}\right)$$

The pseudo-ranges for f1=1575.42 MHz and f2=1227.60 MHz are P1 and P2 as follows respectively. The group delay equation is obtained: The variation of the TEC between the satellite and the receiver depends mainly on the elevation angle of the satellite, called this oblique TEC variation (STEC). For the calculation of the VTEC it is assumed that the ionosphere is a thin film model with a constant reference altitude of the ionosphere (h) whose interval from 350 km to 400 km (Klobuchar, 1996). For our modeling (Amory-Mazaudier et al., 2017), we assume that h=400 km and from the DCB of the satellite and the receiver, we can estimate the value of the TEC absolute. The VTEC varies in time and space and depends on solar activity, receiver position and satellite elevation angle. We used the following equation to convert STEC in VTEC:

$$\mathrm{STEC} = \mathrm{VTEC}\sqrt{1 - \left(\frac{R_T}{R_T + h}\cos\theta\right)^2}$$

R_T = 6371 km is the average radius of the earth, θ: the elevation angle of the satellite (Titheridge, 1972).

2.2 Auxiliary data and characterization of the data sample

To characterize the global context we used the solar index F10.7 cm as an indicator of solar activity (Tapping, 2013).

Figure 2 illustrates the variation of the F10.7 cm solar flux index during the SC#24. Red curve corresponds to the smoothing and blue curves to the monthly mean value of the F10.7 cm solar flux respectively.

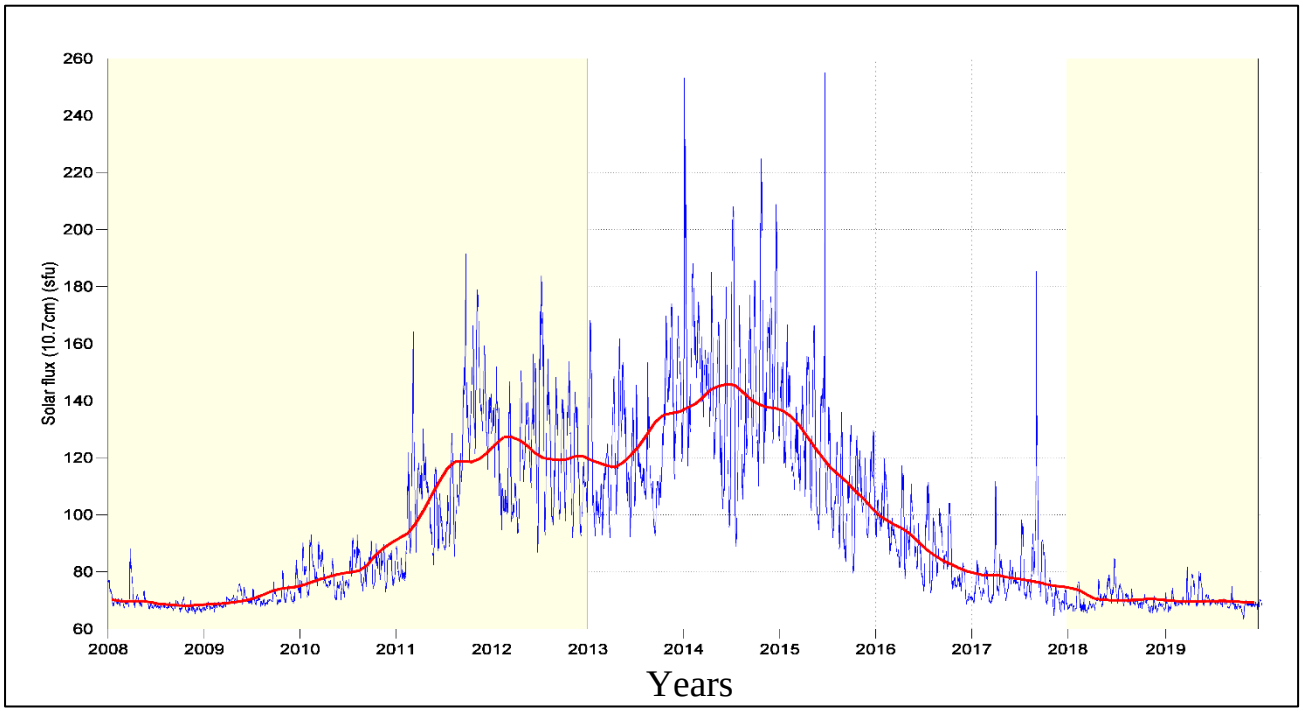

Fig 2. Solar flux variation during the sunspot cycle 24.

3. VTEC Variations: Results and discussion

3.1 Annual VTEC variations

Figures 3, 4, 5 illustrate the VTEC annual variations at low latitude from 2013 to 2017 in American sector (fig.3), Europe-African sector (fig.4) and Asian sector (fig.5). Each map is built by using all the data provided by each station for each year of the study period. Thus, for the 19 stations, 95 annual maps are obtained. On the 3D maps generated, the abscissa axis represents the month of the year, the ordinate axis displays 24 local hours. The color scale represents the VTEC values in TEC units. In this study, the year will be divided into geomagnetic seasons (Lloyd, 1871). The summer includes the months of May, June, July and August; the winter includes the months of November, December, January and February. The spring is composed of the months of March-April and the autumn of September and October All maps show that the daily VTEC values during the study period are significantly higher during the days than during the nights. The maximum VTEC values are recorded during the spring periods, followed by those recorded during the fall. Rishbeth et al., (2000) found the same results. Figures 3, 4 and 5 highlight that VTEC increases during day and decreases slowly during the night. VTEC goes through a minimum before sunrise, and then grows fast enough to reach a maximum around 15.00 LT. The curves show that the decline in the afternoon of the VTEC is faster than the growth in the morning. At sunrise, the term production, i.e. the creation of free electrons under the action of EUV, UV and X-ray radiation, is fast. The time of the daytime maximum is shifted by about 2 hours from the maximum position of the sun, which causes a slight effect of sunset during the VTEC decay period. After sunset, the term of production disappears but ionization is maintained by movement, with time constants governing the disappearance of ionization by recombination or attachment for a long time (Rishbeth, 1971). The observations in Figures 3, 4 and 5 of our study confirm the observations made in Africa by (Shimeis et al., 2014) for Rabat, Libreville and Alexandria. We noted an asymmetry between equinoxes and solstices, observed for all stations and all years during the 2013-2017

periods. The physical mechanisms responsible for semi-annual variation have been among the main scientific objectives in the (Rishbeth and Müller-Wodarg, 2006) ionospheric studies. The main conclusions are as follows: 1) the axial hypothesis (Cortie, 1912): solar wind speed is highest near the equinoxes and lowest at the solstices, 2) the Russell Mac Pherron effect (RM)(Russell and McPherron, 1973): The probability of magnetic reconnection between the interplanetary magnetic field and the terrestrial field lines at the nose of the magnetopause is highest at the equinoxes and lowest at the solstices. 3) The equinox hypothesis (Bartels, 1932; McIntosh, 1959): Kelvin-Helmholtz instability on the sides of the magnetosphere predicts maximum instability at the equinoxes and minimum instability at the solstices. The winter anomaly is due to (1) seasonal change in the O / N2 ratio (Rishbeth and Setty, 1961; Rishbeth and Müller-Wodarg, 2006), (2) the Earth-Sun distance, equinox hypothesis (Yonezawa, 1959; Rishbeth et al., 2000), and (3) waves and tides transmitted from below the thermosphere (Zou et al., 2000). Under study are the distinct mechanisms of formation of the NmF2 winter anomaly (Pavlov and Pavlova, 2005).

Variations in the VTEC during 2013 are stronger during the autumn than during the spring, this is explained by the increase of solar flux during this year (see figure 2). The year 2014 is the year with the maximums of VTEC variation recorded. VTEC exceeds 110 tecu during the spring and autumn. For the years 2015, 2016 and 2017, the maximum VTEC values are recorded during the spring periods, followed by those recorded during the autumn but with a gradual decrease in VTEC values compared to 2014. 2017 is the quietest year, with low VTEC values throughout the year, not exceeding 50 tecu in the spring period. The VTEC values decrease as they approach the magnetic equator in the three sectors of longitude, which is the minimum density of the equatorial fountain. Figures 3, 4 and 5 show that the lowest values of VTEC are for the stations located at latitudes of ± 5° (examples: BRAZ, NKLG and CUSV). The stations furthest from the magnetic equator (examples: OGLA and COCO) have higher densities. This fact this is explained by the equatorial fountain, which consists of two peaks ionization at geomagnetic latitudes +/- 15/20° and a trough of ionization around the geomagnetic equator (Henderson et al., 2005).

Figure 3, 4 and 5 show that the VTEC variation during the spring is higher compared to the autumn in the southern hemisphere (SH) at BRAZ stations in American sector (-170°,-40°):, NKLG and BJCO stations in Europe-African sector (0°, + 40°) : and COCO, TUVA and PNGM stations in Asia sector (+70°, +180°). On the other hand, the VTEC variation during the spring is lower compared to the autumn in northern hemisphere (NH) at KOUR stations in American sector: ADIS and OGLA stations in Europe-African sector and CUSV, IISC and PIMO stations in Asia sector.

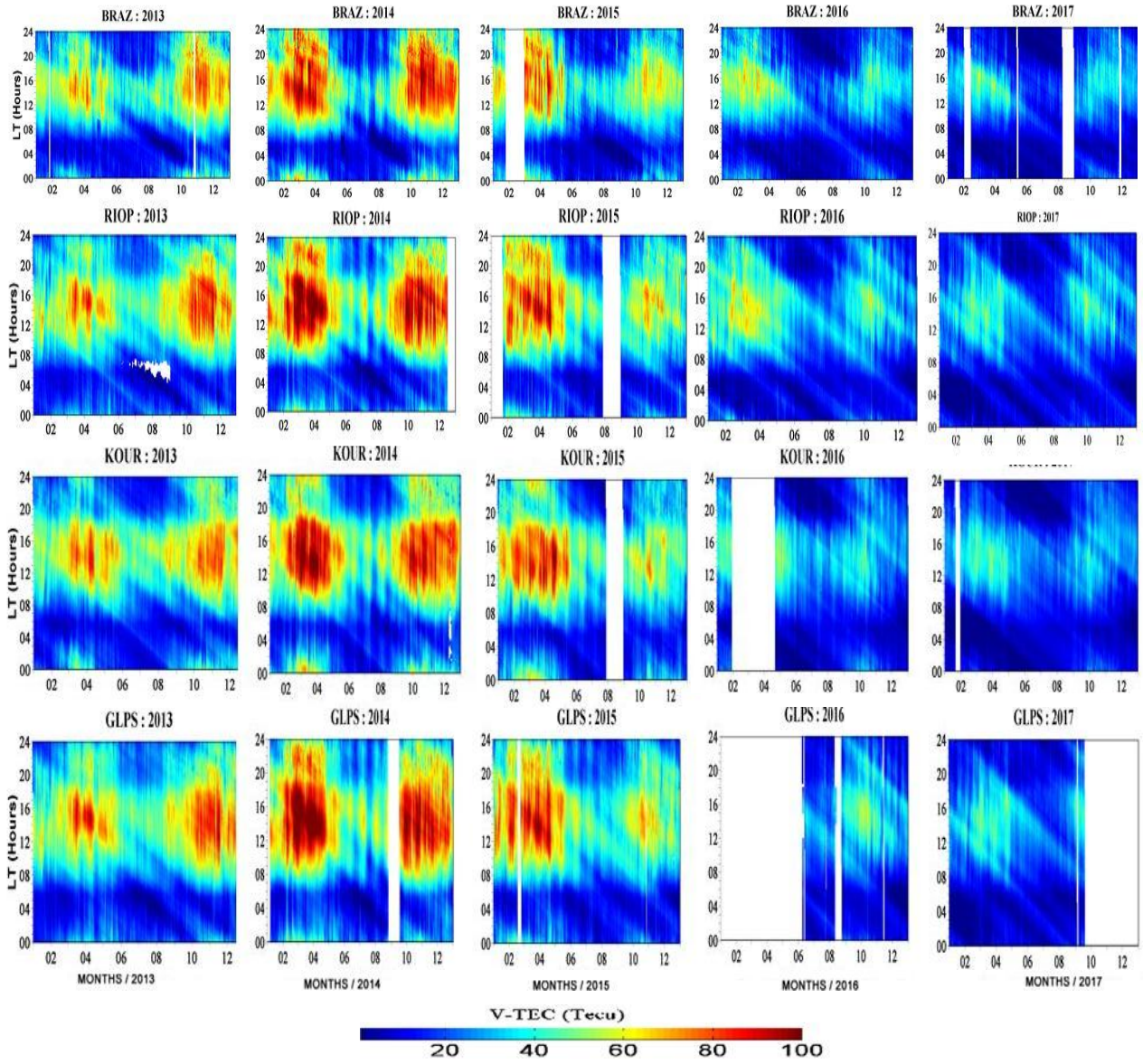

Fig 3. Showing the year-to-year VTEC variations at low latitude from 2013 to 2017 in the American sector. Each map is constructed using all the data provided by each station for each year of the study period. Thus, for the 4 stations: BRAZ, GLPS, RIOP and KOUR, 20 annual maps are obtained. On the generated 3D maps, the x-axis represents the month of the year, the y-axis displays 24 local hours. The color scale represents VTEC values in TEC units.

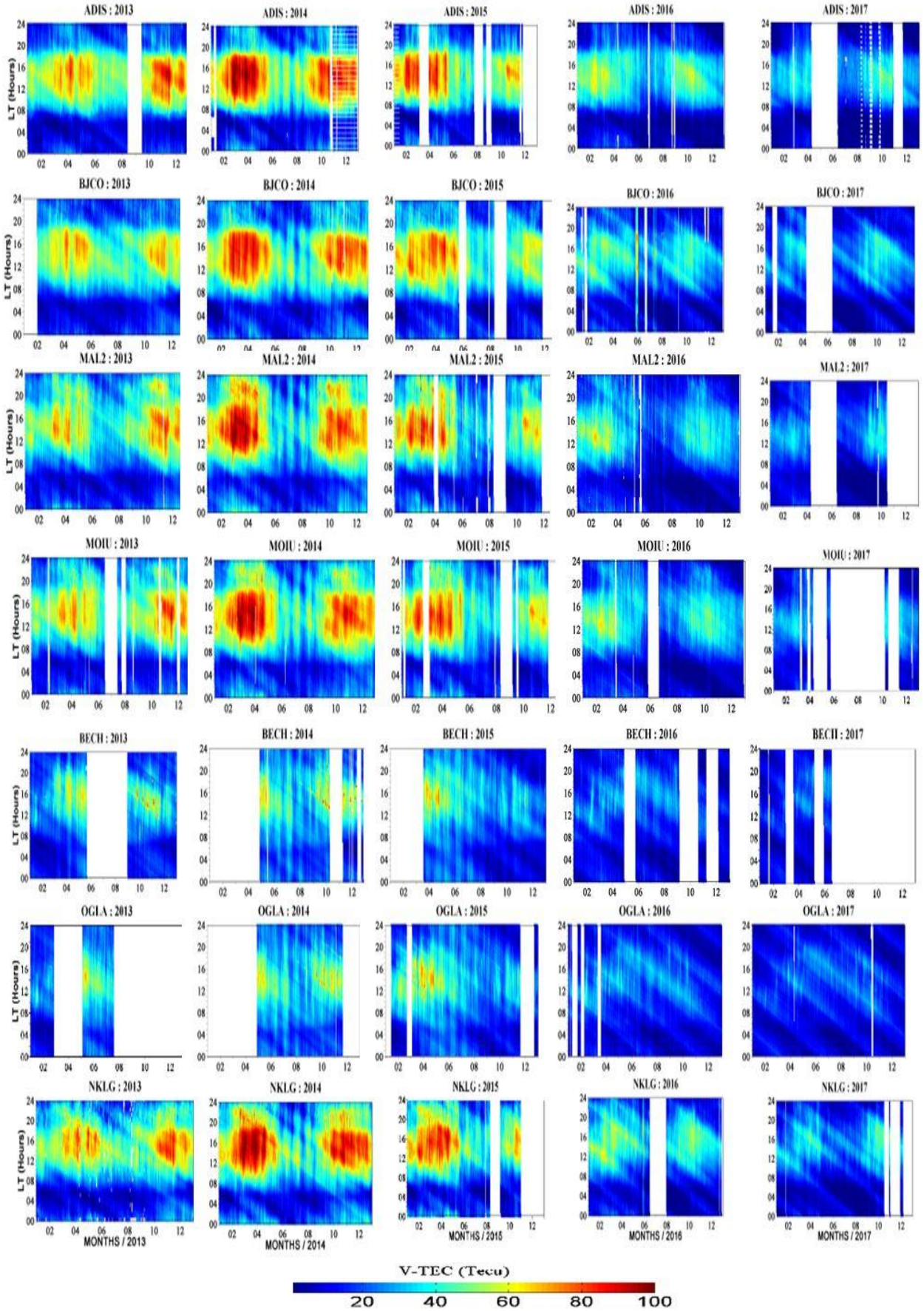

Fig 4. Showing the year-to-year VTEC variations at low latitude from 2013 to 2017 in the Europe-Africa sector. Each map is constructed using all the data provided by each station for each year of the study period. Thus, for the 7 stations: ADIS, BJCO, MAL2, MOIU, NKLG, BECH and OGLA, 35 annual maps are obtained. On the generated 3D maps, the x-axis represents the month of the year, the y-axis displays 24 local hours. The color scale represents the VTEC values in TEC units.

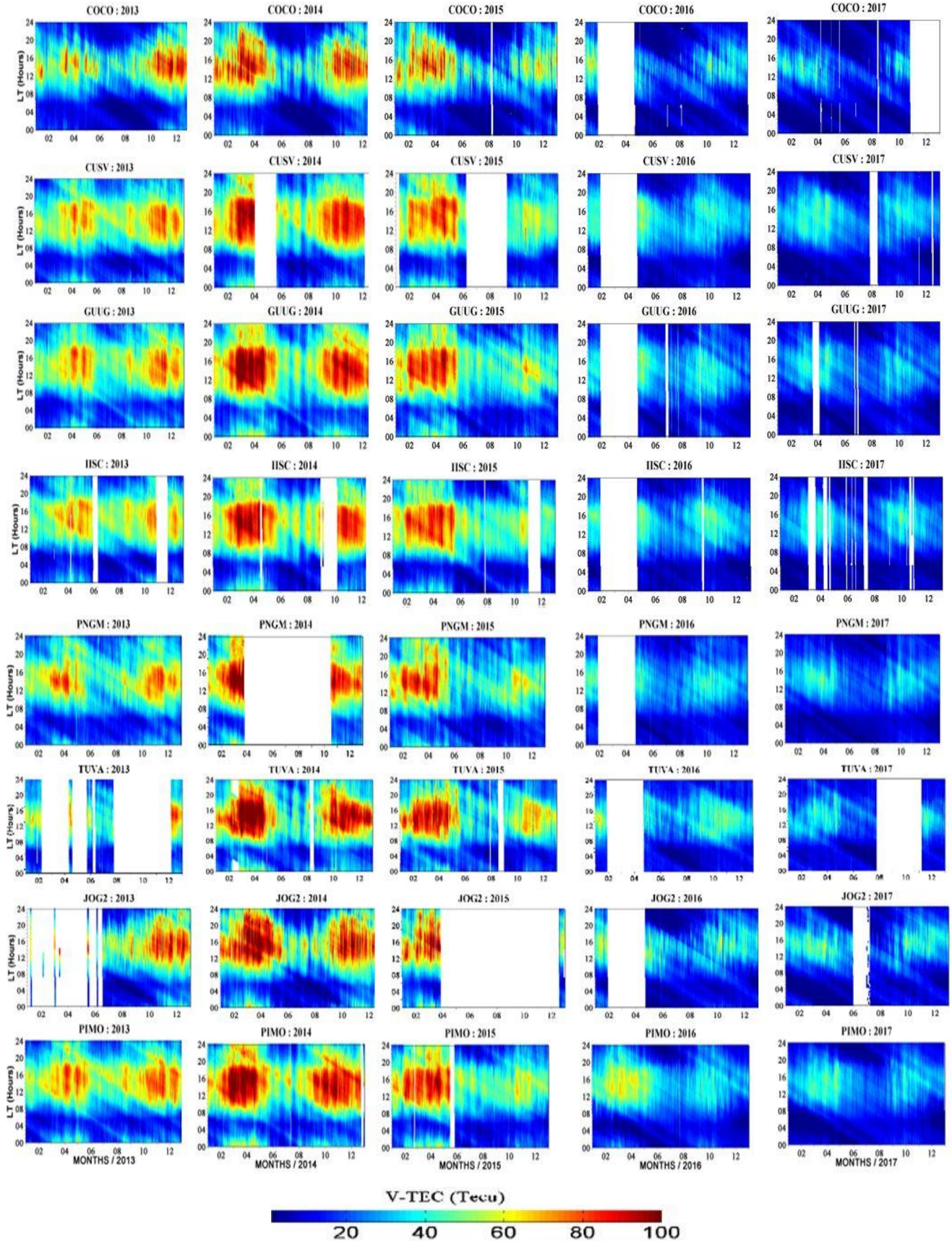

Fig 5. Showing the year-to-year VTEC variations at low latitude from 2013 to 2017 in the Asian sector. Each map is constructed using all data provided by each station for each year of the study period. Thus, for the 8 stations: COCO, CUSV, GUUG, IISC, JOG2, PIMO, PNGM and TUVA, 40 annual maps are obtained. On the generated 3D maps, the x-axis represents the month of the year, the y-axis displays 24 local hours. The color scale represents the VTEC values in TEC units.

3.2 VTEC Seasonal variations

Figure 6a shows the seasonal variations of the VTEC in the three longitude sectors: America, Europe-Africa and Asia (respectively), from 2013 to 2017 study periods, at the 19 GPS stations. On each panel, the abscissa axis represents 24 LT hours. The y-axis displays the VTEC median values (tecu) with different color curves indicating the different seasons given by Lloyd's seasons, (1861). The black color is for winter, the green color for the spring. The summer is plotted in red color and the autumnal in blue color. All curves (Fig. 6a) show that the maximum VTEC values are mainly recorded during the spring, followed by those recorded during the autumnal. The VTEC values during the winter months are higher than those of the summer months in the three sectors of longitude. It is a winter anomaly (Rishbeth and Setty, 1961). Several studies (Zou et al., 2000; Akala et al., 2013) have shown that changes in oxygen and molecular nitrogen concentration were the main cause of seasonal variations and ionospheric parameters. The VTEC seasonal variations in this study describe the six-monthly variations with the equinox maximum and solstice minimum. D'ujanga & Taabu, 2017 reported that, from the sun passing through the equator to the equinox, the March and September undergo the same solar radiation. It is also a well-established fact that March 20 and September 23 are the only times of the year when the solar terminator is perpendicular to the equator, resulting in the maximum equinox. The half-yearly variation was attributed to the effect of the solar zenith angle and the geometry of the magnetic field (Rao et al., 2006; Wu et al., 2008). Another important characteristic of ionospheric parameters (known as equinox asymmetry) is reported in the work of (Bolaji et al., 2012; Akala et al., 2013; D'ujanga and Taabu, 2017). Equinox asymmetry is an important phenomenon at low latitudes; the comparison between African and American equatorial stations carried out during the minimum and upward phases of the SC#24 shows the seasonal values of maximum and minimum VTEC during the March and June, respectively. In the same figure, the seasonal variation of the VTEC is minimal at the December, but maximum at the June. For the three longitudes sectors America, Europe-Africa and Asia, Figure 6a shows that the VTEC variations in the NH are greater compared to the observations of the VTEC in the SH. During the spring in the NH, stations near the magnetic equator have VTEC values in the American sector slightly higher than those observed in the Asian and Europe-African sectors. In the summer period, VTEC values in the Asian sector are slightly higher than those in the American and Europe-African sectors. SH stations near the magnetic equator show that VTEC values in the Asian sector are significantly higher than those in the American and Europe-African sectors during the spring. The VTEC values during the night are slightly higher in the American sector than in Asian and Europe-African. The effect of the equatorial anomaly is visible on the peaks (time range from 12:00 to 16:00 in TL). During this time period, the electron density increases under the effect of the equatorial fountain is visible by the increase in the slope of the VTEC variations, meaning the increase in its values.

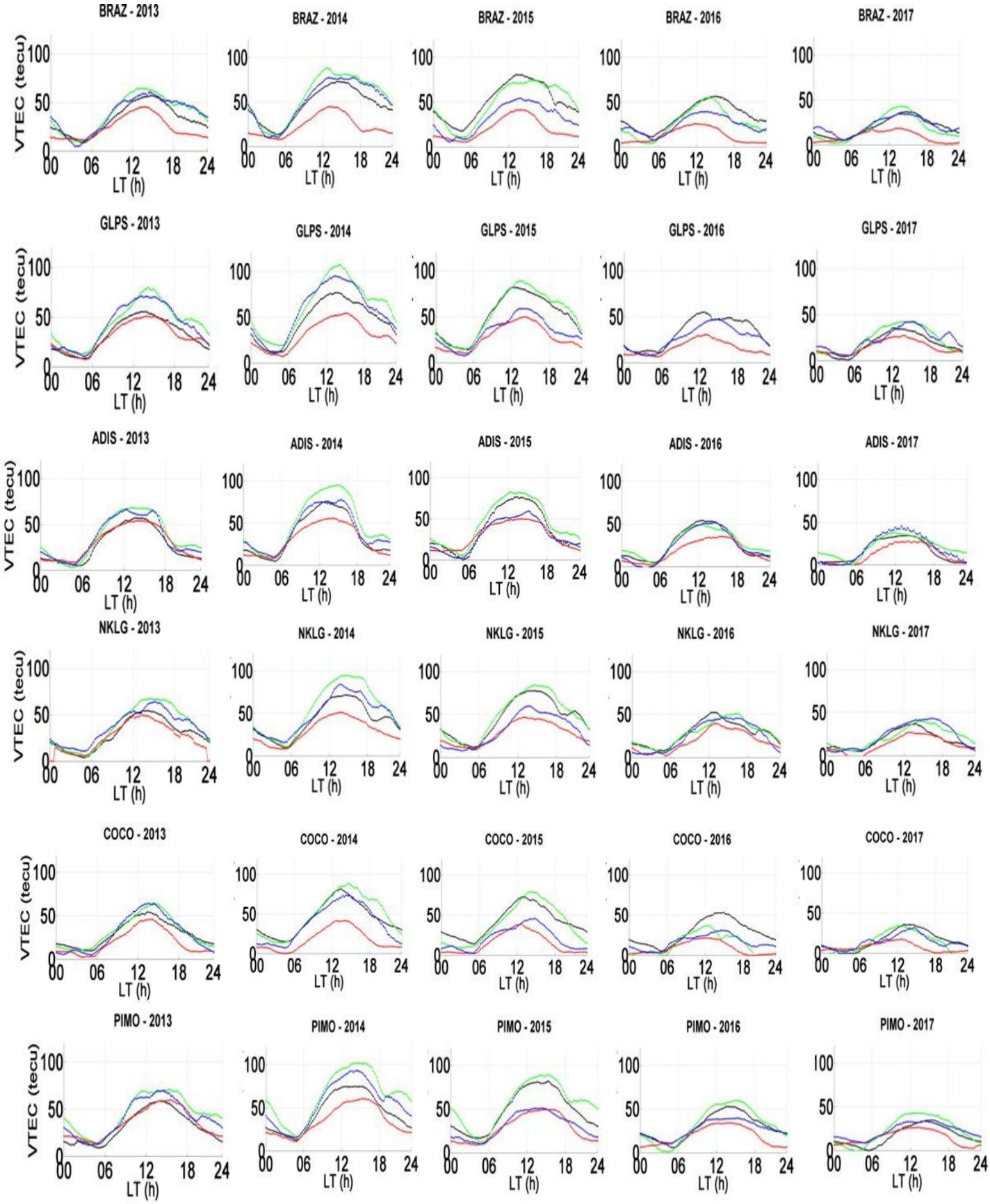

Fig 6a. shows the seasonal variations of the VTEC in the three longitude sectors: America (BRAZ, GLPS), Europe-Africa (ADIS, NKLG) and Asia (COCO, PIMO) (respectively), from 2013 to 2017 study periods, at the 19 GPS stations. On each panel, the abscissa axis represents 24 LT hours. The y-axis displays the VTEC median values (tecu) with different color curves indicating the different seasons given by Lloyd's seasons, (1861).

The figure 6b shows the data dispersion for two stations NKLG and BRAZ located at the southern crest of the EIA, calculated by standard deviation over the five years 2013-2017.
Our conclusion on the variability of the standard deviation (Fig.6b) is as follows:
- Low values at night, between 0 and 5 tecu.
- More daylight values at the spring of 2014 and 2015.
- The standard deviation is approximately 16 tecu between 12 and 22 TL.
- In 2015, the peak is lower at the BRAZ.
- The maximum at the fall in 2014 is more limited in time (~14 TL at NKLG, ~21 TL at the BRAZ). The one in 2015 is significantly lower.
- The diurnal standard deviation declines sharply after mid-2016 to night values.
Variations in the standard deviation strongly follow the TEC levels.

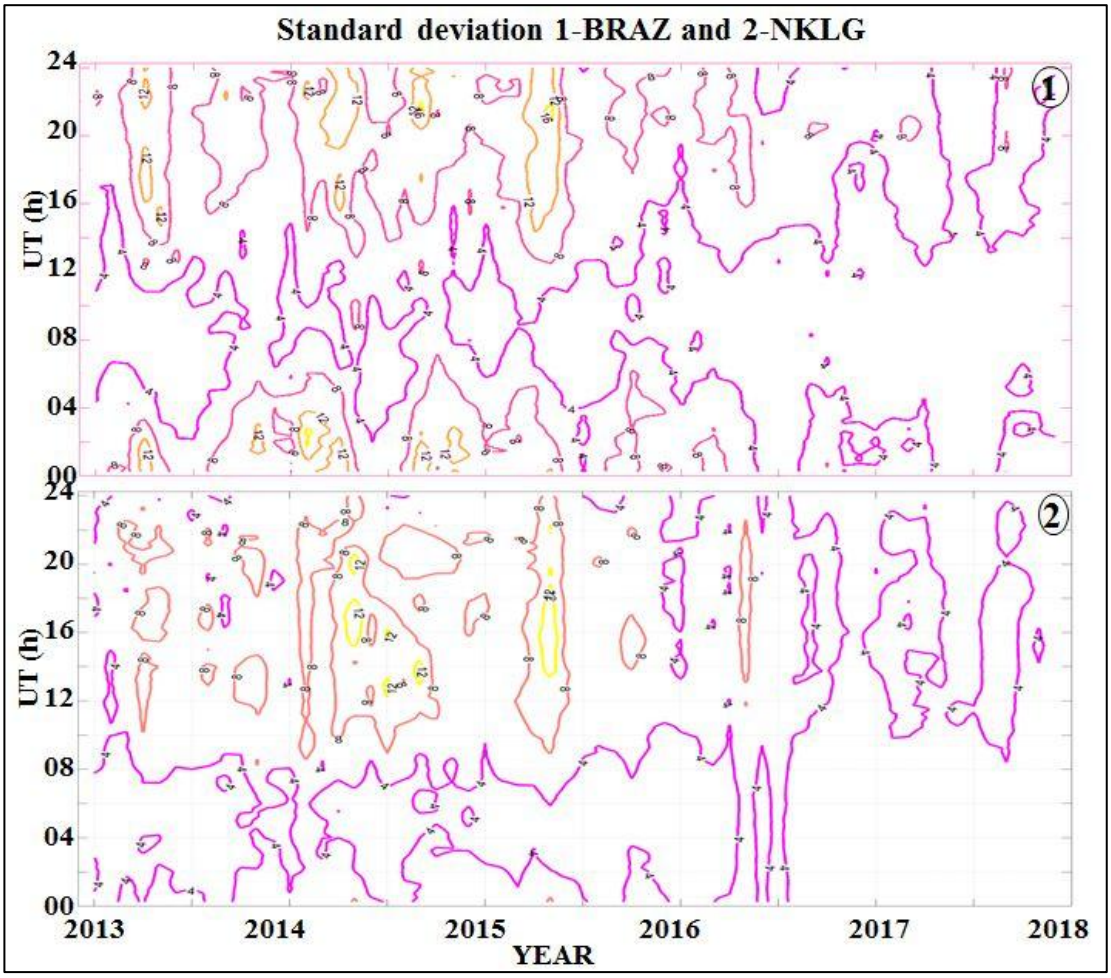

Fig 6b. Data dispersion for two stations BRAZ and NKLG located at the southern crest of the EIA, calculated by standard deviation over the five years 2013-2017.

4. Statistical analysis

4.1 Shape of the VTEC curves

The VTEC seasonal variation curves (Fig 7) reveal three types of morphologies which can be defined as follow: 1) two maximum peaks, 2) bell-shaped curves representing a single peak and 3) plateau-shaped variations.

There are many studies describing the physics of different shapes of TEC curves in the EIA sector in Africa. They can be recorded at the strength, presence or absence of electric currents in the equatorial ionosphere (equatorial electrojet and equatorial counter-electrojet), by reference to the daily variation of electric current over time under calm weather conditions (Vassal, 1982a, 1982b). The three different curves: The 2 Max curve called the noon bite profile, which expresses the signature of a strong electrojet, and the Bell curve called the dome profile and the plateau curve. These two profiles characterize the absence of electrojet (Zoundi et al., 2012; Gyébré et al., 2018).

Studies were conducted on the diurnal behavior of NmF2, using databases of several solar cycles (20,21,22) at Ouagadougou/ Burkina Faso, near the magnetic equator (Ouattara et al., 2009; Ouattara and Amory-Mazaudier, 2012) and at Phu Thuy /Vietnam at the northern crest of the equatorial fountain in Vietnam (Pham Thi Thu et al., 2011).

These statistical studies have shown that near the magnetic equator statistically we find the shape of the 2 max, and at the crest we statistically find the bell shape.

The geomagnetic activity strongly modifies the diurnal behavior of the ionosphere (VTEC or NmF2).

In our case we have averaged all the days together and therefore we do not analyze the effect of magnetic activity. Pham et al (2011) showed that the diurnal variation averaged over all days (magnetic calm and magnetic disturbed) is similar to that averaged over magnetically calm days. In fact, more than 2/3 of the days are calm days (Legrand and Simon, 1989) and the disturbances are distributed randomly during the day. Our observations are made during a weak solar cycle and therefore with a weak equatorial electrojet this explains that the bell shape dominates (see figure 7) In order to better visualize the morphology of the VTEC seasonal variations, we present a statistical analysis based on the VTEC median variations. Figure 7 presents the occurrence of different types of curves shape for the three longitude sectors. Blue color represents the bell curves, which are the most frequent in all the longitude sectors. Green color corresponds to the curves with a double peak, which are slightly more important in the America sector. The plateau curves are in red and show the same occurrence in three longitude sectors. Finally, we observe practically the same distribution of the different classes of VTEC variations in the three sectors of longitude.

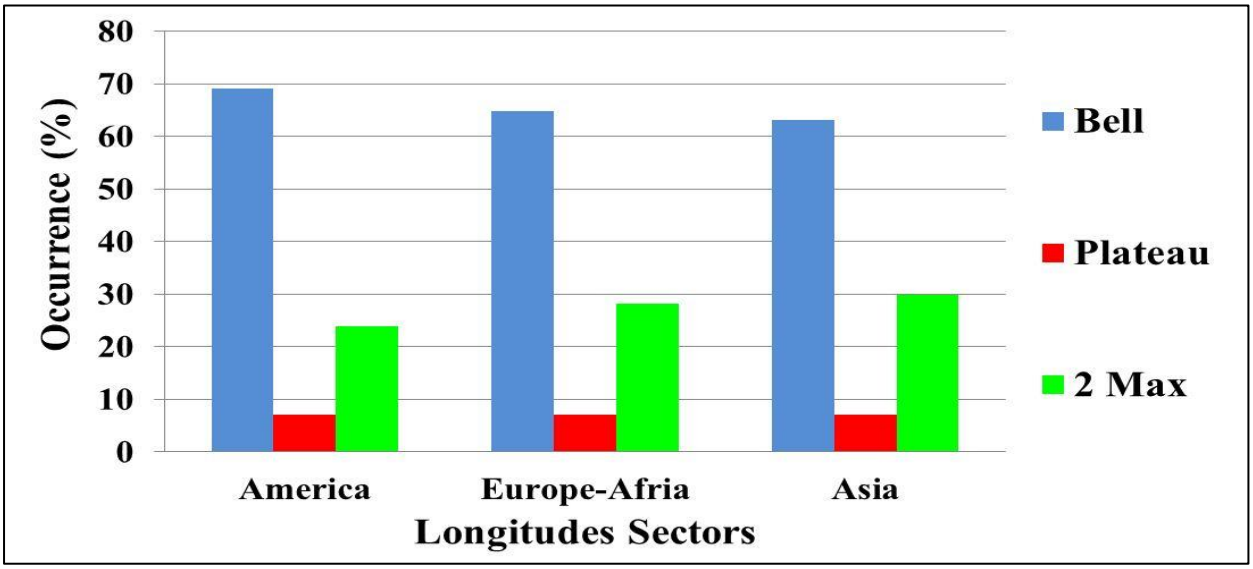

Fig 7. Characteristic of the nature of the variation of VTECs. We select three different curves: Curve 2 Max called the Midday Bite Profile, which expresses the signature of a strong electrojet, and Bell's curve called the Dome Profile and Plateau Curve. These two profiles characterize the absence of electrojet.

4.2 Comparative amplitude of the seasonal VTEC

The VTEC median variations are used to assess the statistical occurrence of comparative VTEC seasonal variations from 2013 to 2017 in the three longitude sectors.

We illustrate in figure 8, the different seasons noted as follows: VTEC amplitude in spring = Sp, VTEC amplitude in autumnal = Au, VTEC amplitude in winter = Wi, VTEC amplitude in summer = Su. The statistical study reveals several classes:

Class 1, in blue (Sp > Au > Wi > Su) shows that the America sector has the highest VTEC values compared to the Asia and Europe-Africa sectors. The highest class 1 in all sectors shows that the spring weighting VTEC values are higher compared to the autumn (between 30% and 55%).

For *class 2*, in dark green (Sp > Wi > Au > Su), the highest VTEC values are found in the America sector, followed by an equivalence of VTEC values between the two sectors Europe-Africa and Asia. This shows that the VTEC values are higher in spring than in winter.

Class 3 in yellow (Au > Sp > Wi > Su), indicates a very high intensity at the VTEC values in the Europe-Africa sector, which are reduced by about half in the America and Asia sectors. This behavior shows that the value of the VTEC weighting autumn is higher compared to Spring.

The two *classes 4* in red (Sp > Au > Su > Wi) and *5* in green (Au > Wi > Sp > Su) display that VTEC values are highest in the Asia sector, followed by a sharp decrease in the Europe-Africa sector and disappear completely in the America sector. Class 4 shows that the spring weighting VTEC values are higher than the autumn values, compared to the class preceding the winter weighting VTEC values. Class 5 shows that the Fall VTEC values are higher than the Winter VTEC values.

Class 6 in brown (Wi > Sp > Au > Su) shows that the VTEC values are quite close with higher values in the Asian sector, which gradually decrease in the American and Europe-Africa sectors. It shows that the winter weighted VTEC values are higher compared to spring.

Class 7 in grey (Wi > Au > Sp > Su) shows that the VTEC values are fairly close with higher values in the American sector, which are gradually decreasing in the American and Europe-Africa sectors. It specifies that the VTEC values are higher in the winter weighting compared to autumn.

All classes, except class 4 show a higher value of VTEC in winter than in summer that corresponds to the winter anomaly (Rishbeth and Müller-Wodarg, 2006).

The class 4 groups together cases for which the winter anomaly does not exist: the winter anomaly is still present in the America sector since class 4 is zero. The winter anomaly is less present in the Asia sector (class 4 > 10%) than in Europe Africa sector (class 4 < 5%)

The sum of classes 1+2+3+5+6+7, concerning the occurrence of the winter anomaly, is 100% for America sector, 95 % for Europe Africa sector ad 89 % for Asia sector. These results show the longitudinal variation in the presence of the winter anomaly in the EIA region.

Classes 1, 2, 4 and 6 bring together the cases for which VTEC at the spring is stronger than VTEC at the autumn. The sum of the occurrences in the four classes, in the America sector is in 84% of cases that the VTEC spring is stronger than VTEC Autumn. In the Europe Africa sector, this is true in 66% of the cases, and in the Asian sector for 83% of the cases. These results show a longitudinal variation in the Spring-Autumn VTEC asymmetry in the EIA region.

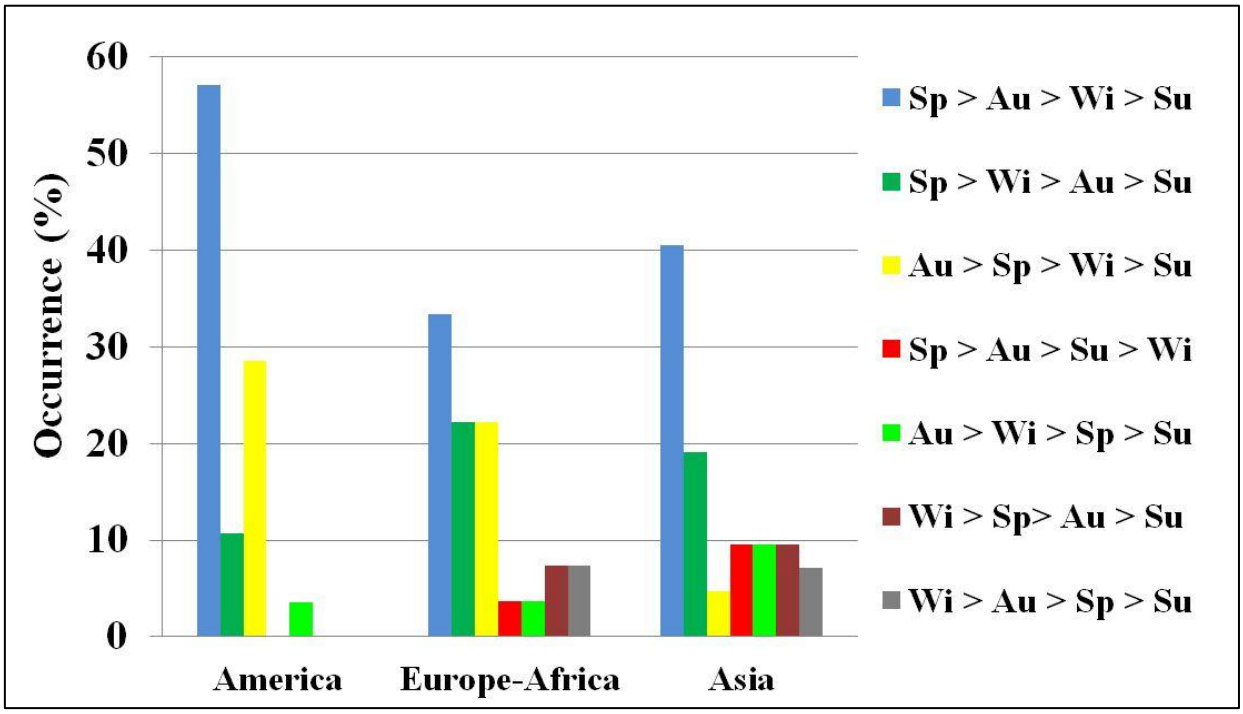

Fig 8. Characteristics of the variations according to the seasons: Sp=spring, Au=Autumn, Wi=Winter, Su=Summer.

Figure 9 shows a difference between the spring and autumn VTEC maximums for the years 2013 to 2017. The dashed black curve in each panel represents the difference in solar flux between spring and autumn.

- During the years 2013 and 2014 (ascending and maximum phase) the difference between spring and autumn (SA) is not explained by the difference in solar flux.
- During the year 2015 the high difference SA is pretty well explained by the solar flux difference.
- During the decreasing phase of the 2016-2017 Solar Flux the asymmetry SA is explained by the solar flux at the equator and on the southern crest (except at BRAZ station). On the northern crest contrast, the SA asymmetry is not explained by the Solar Flux. There is more dispersion on the north crest.

For the right-hand panels concerning the longitude sectors

- In 2013 and 2014 the SA asymmetry is not explained by the solar flux whatever the sector of longitude.
- In 2016 and 2017, the SA asymmetry is well explained by the solar flux in the Europe-Africa sector and in the Asia sector (except for the COCO station).
- For the America sector there is more dispersion and the SA asymmetry is not fully explained by the solar flux.

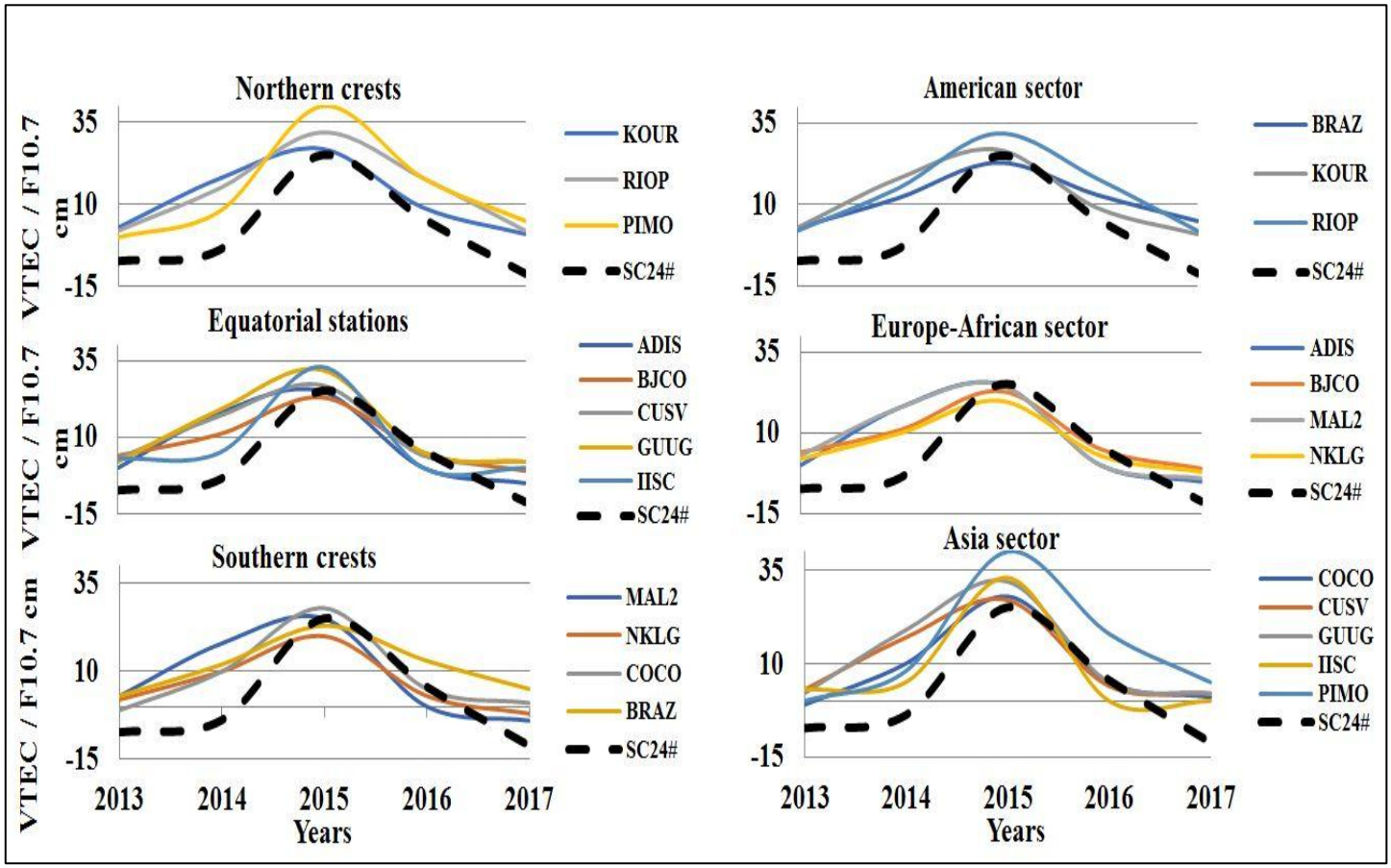

Fig 9. Differences between the spring and Autumn VTEC maximums for the years 2013 to 2017. The dashed black curve in each panel represents the difference in solar flux between spring and autumn. The right-hand panels are for longitude sectors and the left-hand panels for the two crests and the equator

4.3 Night-time VTEC enhancements

Recall that a third ionization peak is observed on almost all figures (3-5), marked by an increase in the VTEC value around 19:00 LT.

Figure 10 describes in detail the occurrence of this increase in the nocturnal VTEC value during the study period from 2013 to 2017. Three panels make up this figure: 1) the latitudinal occurrence of the nocturnal peak (northern and southern crests and equator), 2) the longitudinal occurrence of the nocturnal peak (American, European-African and Asian longitude sectors) and 3) the seasonal occurrence of the nocturnal peak (winter, spring, summer and autumn).

1) The occurrence of nighttime VTEC peaks for North Crest stations is greater in 2014 and 2016 than in other years. For stations closest to the equator the occurrence is highest in 2013 and 2015. For stations on the southern ridge the maximum occurrence is observed in 2017.

2) The longitudinal nocturnal peak occurrence of the VTEC is more important in the Europe-Africa and America sectors during the 5 years (2013-2017), with an occurrence equal to (~75%) in 2014. During the year 2017, the nocturnal peak of VTEC is most frequently observed in the Europe-Africa (~30% of cases), America (~25% of cases) and Asia (~7% of cases) sectors. In the year 2015, we observe an asymmetrical appearance of the VTEC nocturnal peak (~50%) in the three longitude sectors.

3) The seasonal occurrence of the nocturnal VTEC peak is greater during the spring and autumn compared to the winter and summer from 2013 to 2017. The occurrence of the nocturnal VTEC peak during the summer remains relatively constant over 4 years (2013-2016), which is followed by a completely absent occurrence in 2017. In comparison, the occurrence of the VTEC nocturnal peak during the winter is decreasing over the 5 years of the study. It was also noted that the nocturnal maximum of the VTEC is generally higher in the autumn or equal to the nocturnal maximum of the VTEC in the spring. In 2013 and 2017, the maximum occurrence of the nocturnal peak is observed during the winter. The occurrence of the nocturnal peak in all seasons is in the 0-60% range, but the year 2017 differs significantly from the trend of previous years.

In Figure 10, we have added the monthly solar flux variation of SC24# as a dashed line. We noted 3 essential characteristics: the occurrence of the nocturnal peak follows globally the solar cycle. The occurrence of the nocturnal peak is generally strongest at the equinoxes than at the solstices. The occurrence of the nocturnal peak is stronger in the Europe-Africa and America sectors than in the Asia sector.

Although increases in nocturnal VTEC have been observed previously, there is no general agreement on their origin (Horvath and Essex, 2000). These increases in VTEC have a common source, the westward directed electric field.(Horvath and Essex, 2003; Chen et al., 2008) found that the VTEC provided additional information on the formation of nocturnal peaks: VTEC enhancement occurs mainly in the region of the equatorial anomaly, most often in spring and autumn, but rarely in summer. The occurrence of VTEC strengthening is not significantly dependent on the geomagnetic state.

In our study, this VTEC peak occurs around 19 LT, i.e. just after the PRE, we use the study by (Fejer et al., 2008) that corresponds to this local time.

Fejer et al (2008) characterized the vertical drift of the plasma (E x B) measured by the ROCSAT satellite: 1) E x B varies with the solar cycle (figure 7 of (Fejer et al., 2008)), 2) E x B is more important for the equinoxes than for the solstices (figure 6 of (Fejer et al., 2008)) and 3) E x B varies with longitude is stronger during the equinoxes in the Europe-Africa and America sectors than the Asia sector (Figure 8 of (Fejer et al., 2008)).

The occurrence of the nocturnal peak observed around 19 LT has the same characteristics as the vertical drift E x B with regard to the solar cycle, season and longitude. Thus, it seems that the occurrence of the nocturnal peak is well related to the PRE at the origin of the scintillations of the GNSS signal.

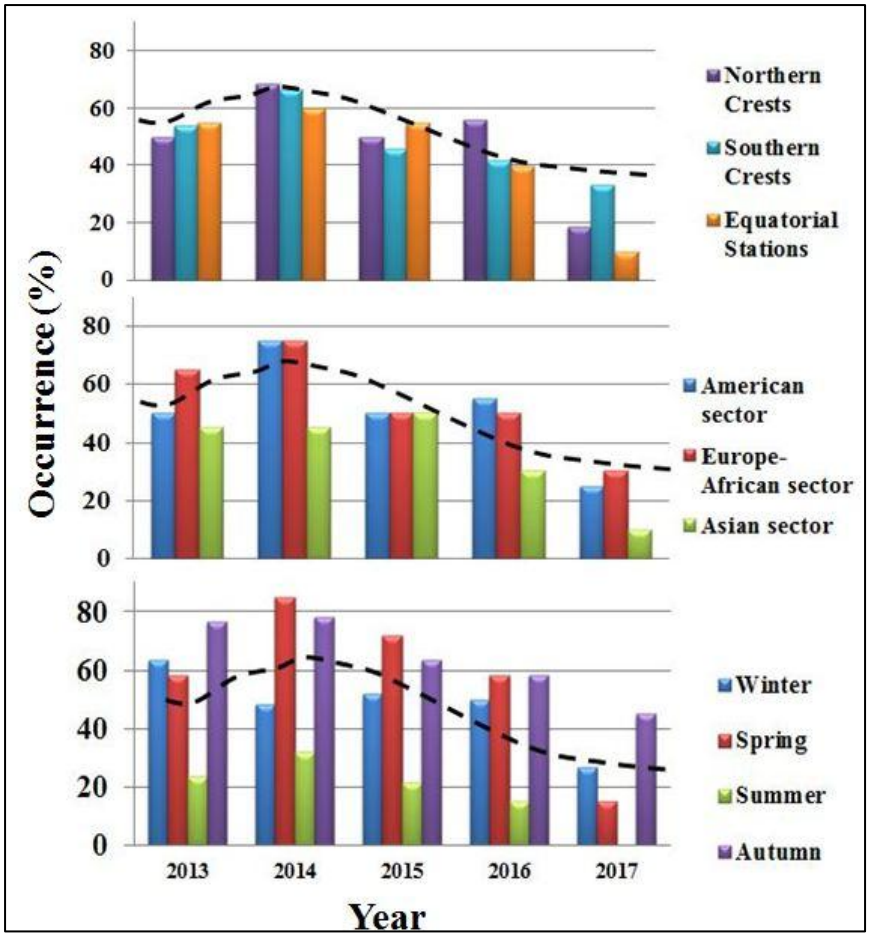

Fig 10. Fig.10. Occurrences of the nocturnal peak of VTEC from 2013 to 2017, panel 1 : latitudinal occurrences, panel 2 longitudinal occurrences and panel 3: seasonal occurrences (winter, spring, summer and autumn).

5. Conclusion

This study includes a morphological analysis of regular variations in ionization during solar activities: daytime variations, seasonal variations and variations based on the 24th solar cycle, obtained by processing GPS data from stations in the Americas, Europe-Africa and Asia sectors. Our analysis focused on the diurnal, seasonal and solar cycle variations of VTECs under local ionospheric conditions during the different phases of the solar cycle 24. Our results highlight that:

- The daily VTEC maximum values were registered between 14:00 and 16:00 LT and the minimum values between 4:00 and 6:00 LT. Double ionization peak in the morning and evening is observed in VTEC annual variations (Fig. 3, 4 and 5), due to the proximity of the stations of the equatorial fountain. As expected, the diurnal variation amplitude of the VTEC depends on the phase of the solar cycle. This is well known the fact that total ionization depends on the solar radiation related to the phases of the solar cycle. We have analyzed the variability of the VTEC during increasing phase of the solar cycle 24 observed around 2013-2014 as well as the decreasing phase around 2014-2017. We found that the winter anomaly and the presence of equinoctial peaks are the most pronounced effects in VTECs in the increasing and decreasing phase. A strong asymmetry is detected between equinoxial peaks and the location of peaks occurring in March/April and October/November at maximum in the solar flux variations during the increase phase.

- In all longitude sectors, the highest VTEC values are displayed during the two months of the spring, located after sunrise and before sunset. The lowest values are found during the summer and winter seasons.
- The statistical analysis reveals practically the same distribution of the different classes of VTEC (two peaks, bell-shaped and plateau-shaped) variations in the three sectors of longitude. These observations indicate longitudinal variation in the presence of the winter anomaly in the EIA region. Additionally, we can note a longitudinal variation of the spring-autumn VTEC asymmetry in the EIA region.
- The occurrence of the nocturnal peak observed around 19 LT has the same characteristics as the vertical drift E x B with regard to the solar cycle, season and longitude. Thus, it seems that the occurrence of the nocturnal peak is well related to the PRE at the origin of the scintillations of the GNSS signal. We noted three essential characteristics: (1) the occurrence of the nocturnal peak follows globally the solar cycle. (2) The occurrence of the nocturnal peak is generally strongest at the equinoxes than at the solstices. (3) The occurrence of the nocturnal peak is stronger in the Europe-Africa and America sectors than in the Asia sector.

Acknowledgments

We thank the NASA/GSFC's Space Physics Data Facility's OMNIWeb service for data (indicator of solar activity F10.7cm index and storm activity Dst index) and speed of the solar wind. We are grateful to the International GPS Services (IGS) (ftp://cddis.gsfc.nasa.gov) and National Institute of Cartography and Remote Sensing (INCT) for the data of the ground-based GPS receivers.

Author thanks the ISSI-Bern International Team of 'Why Ionospheric Dynamics and Structure Behave Differently in The African Sector?' (the team leaders E. Yizengaw & K. Groves) for valuable discussion about part of the result that are included in this paper"

Reference

Adohi, B. P., Vila, P. M., Amory-Mazaudier, C., & Petitdidier, M. (2008). Equinox transition at the magnetic equator in Africa: analysis of ESF ionograms. Annales Geophysicae, Vol. 26, No. 7, pp. 1777-1792.

Akala, A. O., Seemala, G. K., Doherty, P. H., Valladares, C. E., Carrano, C. S., Espinoza, J., & Oluyo, S. (2013). Comparison of equatorial GPS-TEC observations over an African station and an American station during the minimum and ascending phases of solar cycle 24. Annales Geophysicae , Vol. 31, No. 11, pp. 2085-2096.

Amory-Mazaudier, C., Fleury, R., Gadimova, S., & Touzani, A. (2017). Space Weather, from the Sun to the Earth, the key role of GNSS. Part II: Training on daily Global Positioning System (GPS) data. Coordinates, 13(3), pp 31-36.

Amory-Mazaudier, C., Vila, P., Achache, J., Achy-Seka, A., Albouy, Y., Blanc, E., & Vassal, J. (1993). International Equatorial Electrojet Year: The African Sector. Revista Brasileira de Geofísica, 11, 303-317.

Appleton, E. V. (1946). Two anomalies in the ionosphere. Nature, 157(3995), 691-691.

Pham Thi Thu, H., Amory-Mazaudier, C., & Huy, M. L. (2011). Time variations of the ionosphere at the northern tropical crest of ionization at Phu Thuy, Vietnam. Annales Geophysicae, Vol. 29, No. 1, pp. 197-207.

Bartels, J. (1932). Terrestrial-magnetic activity and its relations to solar phenomena. Terrestrial Magnetism and Atmospheric Electricity, 37(1), 1-52.

Bilitza, D., Altadill, D., Truhlik, V., Shubin, V., Galkin, I., Reinisch, B., & Huang, X. (2017). International Reference Ionosphere 2016: From ionospheric climate to real-time weather predictions. Space Weather, 15(2), 418-429.

Bolaji, O. S., Adeniyi, J. O., Radicella, S. M., & Doherty, P. H. (2012). Variability of total electron content over an equatorial West African station during low solar activity. Radio Science, 47(01), 1-9.

Chapman, S. (1951). The equatorial electrojet as detected from the abnormal electric current distribution above Huancayo, Peru, and elsewhere. Archiv Fuer Meteorologie, Geophysik und Bioklimatologie, Serie A, 4(1), 368-390.

Chen, Y., Ma, G., Huang, W., Shen, H., & Li, J. (2008). Night-time total electron content enhancements at equatorial anomaly region in China. Advances in Space Research, 41(4), 617-623.

Cortie, A. L. (1912). Sun-spots and Terrestrial Magnetic Phenomena, 1898–1911: the Cause of the Annual Variation in Magnetic Disturbances. Monthly Notices of the Royal Astronomical Society, 73(1), 52-60.

D'ujanga, F. M., and Taabu, S. D. (2017). Study on the occurrence characteristics of VHF and L-band ionospheric scintillations over East Africa. Indian Journal of Radio & Space Physics (IJRSP), 43(4-5), 263-273.

Fang, T. W., Fuller-Rowell, T., Yudin, V., Matsuo, T., & Viereck, R. (2018). Quantifying the sources of ionosphere day-to-day variability. Journal of Geophysical Research: Space Physics, 123(11), 9682-9696.

Fejer, B. G., De Paula, E. R., Heelis, R. A., & Hanson, W. B. (1995). Global equatorial ionospheric vertical plasma drifts measured by the AE-E satellite. Journal of Geophysical Research: Space Physics, 100(A4), 5769-5776.

Fejer, B. G., Jensen, J. W., & Su, S. Y. (2008). Seasonal and longitudinal dependence of equatorial disturbance vertical plasma drifts. Geophysical Research Letters, 35(20). https://doi.org/10.1029/2008GL035584

Fejer, B. G., Scherliess, L., & De Paula, E. R. (1999). Effects of the vertical plasma drift velocity on the generation and evolution of equatorial spread F. Journal of Geophysical Research: Space Physics, 104(A9), 19859-19869.

Gyébré, A. M. F., Gnabahou, D. A., & Ouattara, F. (2018). The geomagnetic effects of solar activity as measured at Ouagadougou Station. International Journal of Astronomy and Astrophysics, 8(02), 178.

Henderson, S. B., Swenson, C. M., Christensen, A. B., & Paxton, L. J. (2005). Morphology of the equatorial anomaly and equatorial plasma bubbles using image subspace analysis of Global Ultraviolet Imager data. Journal of Geophysical Research: Space Physics, 110(A11).

Horvath, I., and Essex, E.A., (2000). Investigating the mid-latitude nighttime total electron content (TEC) enhancements and their relation to the low-latitude ionosphere at low sunspot numbers, in: Workshop on the Applications of Radio Science WARS. http://www.sws.bom.gov.au/IPSHosted/NCRS/wars/wars2000/commg/horvath.pdf.

Horvath, I., and Essex, E. A. (2003). Vertical E× B drift velocity variations and associated low-latitude ionospheric irregularities investigated with the TOPEX and GPS satellite data. Annales Geophysicae, Vol. 21, No. 4, pp. 1017-1030.

Immel, T.J., Sagawa, E., England, S.L., Henderson, S.B., Hagan, M.E., Mende, S.B., Frey, H.U., Swenson, C.M., Paxton, L.J., 2006. Control of equatorial ionospheric morphology by atmospheric tides. Geophys. Res. Lett. 33, L15108. https://doi.org/10.1029/2006GL026161.

Jin, S., Jin, R., & Kutoglu, H. (2017). Positive and negative ionospheric responses to the March 2015 geomagnetic storm from BDS observations. Journal of Geodesy, 91(6), 613-626.

Kelley, M. (1989). The Earth's ionosphere: Plasma physics and electrodynamics, Int. Geophys. Ser, 43, 437-455.

Klobuchar, J. (1996). Ionospheric Effects on GPS. Global Positioning System: Theory and Applications, Chapter 12, vol 1, 485-515

Le, H., Liu, L., Chen, Y., & Wan, W. (2013). Statistical analysis of ionospheric responses to solar flares in the solar cycle 23. Journal of Geophysical Research: Space Physics, 118(1), 576-582.

Legrand, J. P., and Simon, P. A. (1989). Solar cycle and geomagnetic activity: A review for geophysicists. Part I. The contributions to geomagnetic activity. Annales geophysicae, Vol. 7, No. 6, pp. 565-578.

Lloyd, H. (1871). On earth-currents, and their connexion with the diurnal changes of the horizontal magnetic needle. The Transactions of the Royal Irish Academy, 24, 115-142.

McIntosh, D. H. (1959). On the annual variation of magnetic disturbance. Philosophical Transactions of the Royal Society of London. Series A, Mathematical and Physical Sciences, 251(1001), 525-552.

Namba, S., and Maeda K. I. (1939). Radio wave propagation, 86.

Oladipo, O. A., Adeniyi, J. O., Radicella, S. M., & Obrou, O. K. (2008). Variability of equatorial ionospheric electron density at fixed heights below the F2 peak. Journal of Atmospheric and Solar-Terrestrial Physics, 70(7), 1056-1065.

Olsen, N., Stolle, C., Floberghagen, R., Hulot, G., & Kuvshinov, A. (2016). Swarm science results after 2 years in space. Earth, Planets and Space, 68(1), 1-3.

Ouattara, F., and Amory-Mazaudier, C. (2012). Statistical study of the equatorial F2 layer critical frequency at Ouagadougou during solar cycles 20, 21 and 22, using Legrand and Simon's classification of geomagnetic activity. Journal of Space Weather and Space Climate, 2, A19.

Ouattara, F., Amory-Mazaudier, C., Fleury, R., Lassudrie Duchesne, P., Vila, P., & Petitdidier, M. (2009). West African equatorial ionospheric parameters climatology based on Ouagadougou ionosonde station data from June 1966 to February 1998. Annales Geophysicae ,Vol. 27, No. 6, pp. 2503-2514.

Pavlov, A. V., and Pavlova, N. M. (2005). Causes of the mid-latitude NmF2 winter anomaly at solar maximum. Journal of atmospheric and solar-terrestrial physics, 67(10), 862-877.

Pham Thi Thu, H., Amory-Mazaudier, C., & Huy, M. L. (2011). Time variations of the ionosphere at the northern tropical crest of ionization at Phu Thuy, Vietnam. Annales Geophysicae, Vol. 29, No. 1, pp. 197-207.

Rama Rao, P. V. S., Gopi Krishna, S., Niranjan, K., & Prasad, D. S. V. V. D. (2006). Temporal and spatial variations in TEC using simultaneous measurements from the Indian GPS network of receivers during the low solar activity period of 2004–2005. Annales Geophysicae, Vol. 24, No. 12, pp. 3279-3292.

Rishbeth, H. (1971). Polarization fields produced by winds in the equatorial F-region. Planetary and Space Science, 19(3), 357-369.

Rishbeth, H., & Müller-Wodarg, I. C. F. (2006). Why is there more ionosphere in January than in July? The annual asymmetry in the F2-layer. Annales Geophysicae, Vol. 24, No. 12, pp.3293-3311.

Rishbeth, H., Müller-Wodarg, I. C. F., Zou, L., Fuller-Rowell, T. J., Millward, G. H., Moffett, R. J., & Aylward, A. D. (2000). Annual and semiannual variations in the ionospheric F2-layer: II. Physical discussion. Annales Geophysicae, Vol. 18, No. 8, pp. 945-956.

Rishbeth, H., and Setty, C. S. G. K. (1961). The F-layer at sunrise. Journal of Atmospheric and Terrestrial Physics, 20(4), 263-276

Russell, C. T., and McPherron, R. L. (1973). Semiannual variation of geomagnetic activity. Journal of geophysical research, 78(1), 92-108.

Sardon, E., Rius, A., & Zarraoa, N. (1994). Estimation of the transmitter and receiver differential biases and the ionospheric total electron content from Global Positioning System observations. Radio science, 29(03), 577-586.

Shimeis, A., Amory-Mazaudier, C., Fleury, R., Mahrous, A. M., & Hassan, A. F. (2014). Transient variations of vertical total electron content over some African stations from 2002 to 2012. Advances in Space Research, 2014, vol. 54, no 11, p. 2159-2171.

Tapping, K. F. (2013). The 10.7 cm solar radio flux (F10. 7). Space Weather, 11(7), 394-406.

Thiam, N. M., Ouattara, F., Gnabahou, D. A., Amory-Mazaudier, C., Fleury, R., & Lassudrie-Duchesne, P. (2012). Variation of F2 layer critical frequency with solar cycle at Dakar station. Journal des sciences, 11(2), 16-20.

Titheridge, J. E. (1972). Determination of ionospheric electron content from the Faraday rotation of geostationary satellite signals. Planetary and Space Science, 20(3), 353-369.

Vassal, J. (1982). La variation du champ magnétique et ses relations avec I'électrojet équatorial au Sénégal Oriental. Annales Geophysicae, Vol. 3, pp. 347-355.

Vassal, J. (1982). Electrojet, contre-électrojet et région F à Sarh (Tchad). Géophysique, (19), 3-9.

Woodman, R. F. (1970). Vertical drift velocities and east-west electric fields at the magnetic equator. Journal of Geophysical Research, 75(31), 6249-6259.

Wu, C. C., Liou, K., Shan, S. J., & Tseng, C. L. (2008). Variation of ionospheric total electron content in Taiwan region of the equatorial anomaly from 1994 to 2003. Advances in Space Research, 41(4), 611-616.

Ya'acob, N., Abdullah, M., Ismail, M., & Zaharim, A. (2009). Model validation for total electron content (TEC) at an equatorial region. European Journal of Scientific Research, 28(4), 643-649.

Yonezawa, T. (1959). On the seasonal and non-seasonal annual variations and the semi-annual variation in the noon and midnight electron densities of the F-2 layer in middle latitudes. J. Radio Res. Labs, 6, 293-309.

Zou, L., Rishbeth, H., Müller-Wodarg, I. C. F., Aylward, A. D., Millward, G. H., Fuller-Rowell, T. J., & Moffett, R. J. (2000). Annual and semiannual variations in the ionospheric F2-layer. I. Modelling. Annales Geophysicae, Vol. 18, No. 8, pp. 927-944.

Zoundi, C., Ouattara, F., Fleury, R., Amory-Mazaudier, C., & Lassudrie-Duchesne, P. (2012). Seasonal TEC variability in West Africa equatorial anomaly region. European Journal of Scientific Research, 77(3), 309-319.